

Electron-Hole Symmetry and Magnetic Coupling in Antiferromagnetic LaFeAsO

Z. P. Yin,¹ S. Lebègue,^{1,2} M. J. Han,¹ B. P. Neal,¹ S. Y. Savrasov,¹ and W. E. Pickett¹

¹Department of Physics, University of California Davis, Davis, California 95616, USA

²Laboratoire de Cristallographie et de Modélisation des Matériaux Minéraux et Biologiques, UMR 7036, CNRS-Université Henri Poincaré, B.P. 239, F-54506 Vandoeuvre-lès-Nancy, France

(Received 21 April 2008; published 21 July 2008)

When either electron or hole doped at concentrations $x \sim 0.1$, the LaFeAsO family displays remarkably high temperature superconductivity with T_c up to 55 K. In the most energetically stable $Q_M = (\pi, \pi, 0)$ antiferromagnetic (AFM) phase comprised of tetragonal-symmetry breaking alternating chains of aligned spins, there is a deep pseudogap in the Fe $3d$ states centered at the Fermi energy arising from light carriers ($m^* \sim 0.25$ – 0.33), and very strong magnetophonon coupling is uncovered. Doping (of either sign) beyond $x \sim 0.08$ results in heavy carriers per Fe (by roughly an order of magnitude) with a large Fermi surface. Calculated Fe-Fe transverse exchange couplings $J_{ij}(R)$ reveal that exchange coupling is strongly dependent on both the AFM symmetry and on the Fe-As distance.

DOI: 10.1103/PhysRevLett.101.047001

PACS numbers: 74.70.-b, 71.18.+y, 71.20.-b, 75.25.+z

Since the appearance of copper oxide high temperature superconductors (HTS) two decades ago [1], there has been a determined but underfunded effort to discover related superconductors in two-dimensional (2D) transition metal oxides (TMO), borides, nitrides, etc.,. Promising developments in this area include Li_xNbO_2 , [2], Sr_2RuO_4 , [3] Na_xCoO_2 , [4], and Cu_xTiSe_2 , [5] but all have superconducting critical temperature T_c of 5 K or less. The most striking discovery was that of electron-doped hafnium nitride semiconductor (HfNCl) [6] with $T_c = 25$ K. The other distinctive breakthrough [7], MgB_2 ($T_c = 40$ K), has strong 2D features but contains only s , p elements. Recently, design of possible TMO superconductors has been stimulated by a specific approach outlined by Chaloupka and Khaluillin [8].

The simmering state of superconductor discovery has been reignited by the report of a new class of layered transition metal pnictides $\mathcal{R}\mathcal{T}\text{PnO}$, where \mathcal{R} is a trivalent rare earth ion, \mathcal{T} is a late transition metal ion, and Pn is a pnictogen atom. The breakthrough of $T_c = 26$ K reported [9] for electron-doped $\text{LaFeAsO}_{1-x}\text{F}_x$ ($x \sim 0.05$ – 0.1), followed by the demonstration that hole doping [10] in $\text{La}_{1-x}\text{Sr}_x\text{FeAsO}$ leads to a similar value of T_c . These values of T_c have now been superseded by the finding that replacement of La by lanthanide ions [11–15] results in T_c up to 55 K, substantially higher than in any materials except for the cuprate HTS.

The transport, magnetic, and superconducting properties of $\text{LaFeAsO}_{1-x}\text{F}_x$ depend strongly on carrier concentration [9,10,16]. Most interestingly, a kink is observed [17] in the resistivity of the stoichiometric (“undoped” but conducting) compound, which has been identified with a structural symmetry lowering followed by the onset of antiferromagnetism (AFM). As a result, the original focus on the non-magnetic LaFeAsO compound switched to an AFM ground state, in which the two Fe atoms in the primitive cell have oppositely oriented moments. Because of the structure of

the Fe-As layer, shown in Fig. 1, which itself requires two Fe atoms in the primitive cell, this ordering represents a $Q = 0$ AFM state.

The basic electronic structure of this class of compounds was presented for LaFePO, superconducting at 5 K [18], by Lebègue [19]. The electronic structure of paramagnetic LaFeAsO is similar, and its (actual or incipient) ferromagnetic (FM) instabilities have been described by Singh and

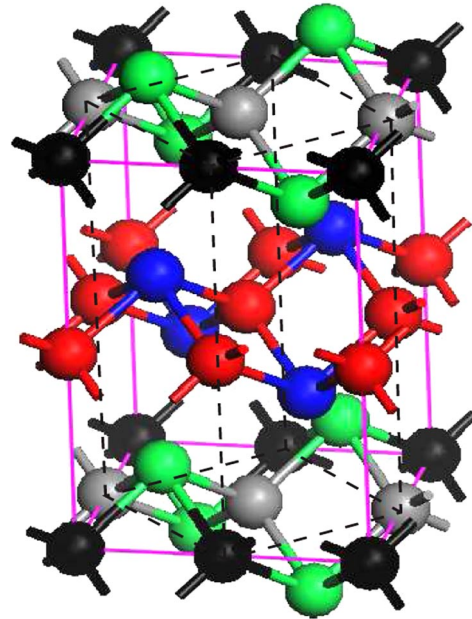


FIG. 1 (color online). The Q_M antiferromagnetic structure of LaFeAsO, with different shades of Fe atoms (top and bottom planes) denoting the opposing directions of spins in the Q_M AFM phase. Fe atoms lie on a square sublattice coordinated tetrahedrally by As atoms, separated by LaO layers (center of figure) of similar structure. The dashed lines indicate the non-magnetic primitive cell.

Du [20], who found that the Fermi level (E_F) lies on the edge of a peak in the density of states (DOS), making the electronic structure strongly electron-hole *asymmetric*. The Fermi surfaces are dominated by zone center and zone corner cylinders, which underlie several models of both magnetic [21] and superconducting [22–25] properties. Cao *et al.* [26] and Ma and Lu [27] demonstrated that a $Q = 0$ AFM state (mentioned above) is energetically favored, but coincidentally (because the electronic structure is substantially different) still leaves E_F on the edge of a DOS peak, i.e., strongly particle-hole asymmetric. In both paramagnetic and $Q = 0$ AFM states a degenerate d_{xz}, d_{yz} pair of Fe orbitals remains roughly half-filled, suggesting possible spontaneous symmetry breaking to eliminate the degeneracy [21,28]. Such degeneracies have attracted attention in transition metal oxides [29].

Subsequently, a $\vec{Q}_M = (\pi, \pi, 0) \sqrt{2} \times \sqrt{2}$ AFM state was uncovered [22,30,31], and reported by Dong *et al.* [30] to be lower still in energy. The state consists of chains of aligned Fe spins along one direction (which we take to be the x axis) of the square Fe sublattice, with alternate chains having opposite spin direction. This \vec{Q}_M ordering is what might be expected from the (approximate) nesting of Fermi surfaces in the primitive cell, but the calculated moments are large ($1.72 \mu_B$ in the $Q = 0$ phase, $1.87 \mu_B$ for Q_M) and thus seems far removed from a “spin density wave” description. Neutron scattering [32] and x-ray diffraction [33] have confirmed this in-plane ordering, and reveal that alternating planes of Fe spins are antialigned, i.e., the true ordering is (π, π, π) . The observed moment is only $\sim 20\%$ of our calculated value, which we tentatively ascribe to strong paramagnetic fluctuations but which clearly requires study.

To prepare for studying the superconducting state, it is necessary first to understand the normal state from which it emerges. Here we analyze the conducting Q_M AFM phase, using results from two all-electron, full potential codes WIEN2K [34] and FPLO [35,36] using the generalized gradient approximation [37] (GGA) functional and the experimentally determined structure. Fixed spin moment (constrained FM) calculations show that the energy is invariant to within 1 meV/Fe for moments in the range $0-0.2 \mu_B/\text{Fe}$, which seems to be consistent with results of Singh and Du [20]. We find the AFM Q_M phase to be energetically favored over the $Q = 0$ AFM phase by ~ 75 meV/Fe, which itself lies 87 meV/Fe below the nonmagnetic phase. This energy difference is large enough that neither the $Q = 0$ AFM, nor the nonmagnetic/FM, phase will be thermally accessible at temperatures of interest. In either AFM phase, the Fe majority states are completely filled; thus, the moment is determined by the occupation of the minority states. From the projected Fe $3d$ density of states (DOS) shown in Fig. 2, calculated from the band structure presented in Fig. 3, the minority states are almost exactly half-filled, giving 7.5 $3d$ electrons and

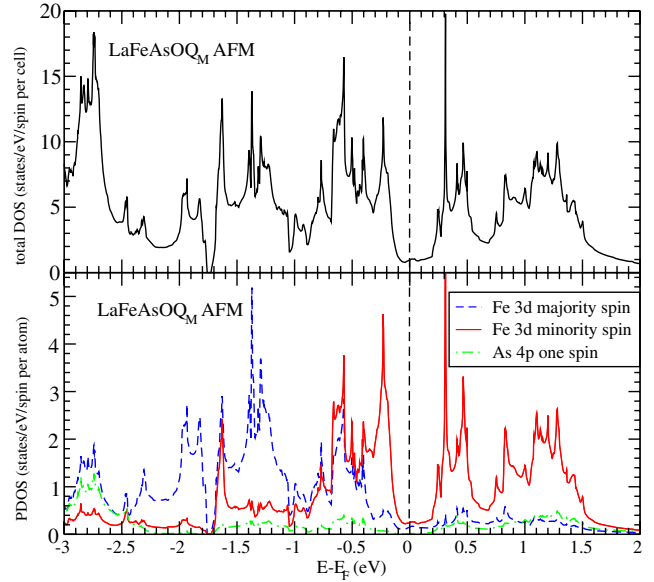


FIG. 2 (color online). Top panel: total DOS for the Q_M AFM phase. Bottom panel: spin resolved Fe $3d$ DOS, showing majority filled and minority half-filled up to the pseudogap, and the As $4p$ DOS.

suggesting an Fe state that is no more than $0.5e$ from neutral. While the center of gravity of As $4p$ weight lies below that of Fe $3d$ bands, there is mixing of these two characters on both sides of E_F , and the As $4p$ states are certainly unfilled.

Notably, the band structure and DOS is characterized by a pseudogap straddling E_F , seemingly separating bonding and antibonding bands and closing only in a small region along the Γ - Y line near Γ . Since the moments, and hence the exchange energies, of the two AFM phases are very similar, the energy gain in the Q_M phase can be ascribed to the formation of the pseudogap. The system could be considered as *metallic* rather than semimetallic, in the sense that there are two dispersive bands crossing E_F along Γ - Y . One is 1.3 eV wide, comprised of Fe $d_{xy} + \text{As}p_z$ character, the other of d_{yz} character is 0.9 eV wide. A third narrower (0.4 eV) band of $3d_{x^2-y^2}$ character crosses E_F near Γ . The intersecting of the dispersive bands along Γ - Y is such as to leave only two small distinct 2D Fermi surfaces, shown in Fig. 4: an elliptical hole cylinder at Γ containing ~ 0.03 holes, and two symmetrically placed near-circular electron tubes midway along the Γ - Y axis. In the sense that the Fermi surfaces are small, the state is semimetallic. The bands near E_F have k_z dispersion of no more than 25 meV.

The d_{xz}, d_{yz} degeneracy is broken by the chains of aligned Fe spins in the Q_M phase. The rough characterization for the minority Fe orbitals is that d_{z^2} and $d_{x^2-y^2}$ states are partially filled, d_{xy} and d_{xz} states are empty, the d_{yz} states are mostly filled but give rise to the hole Fermi surfaces. (Note that here the $x - y$ coordinate system is

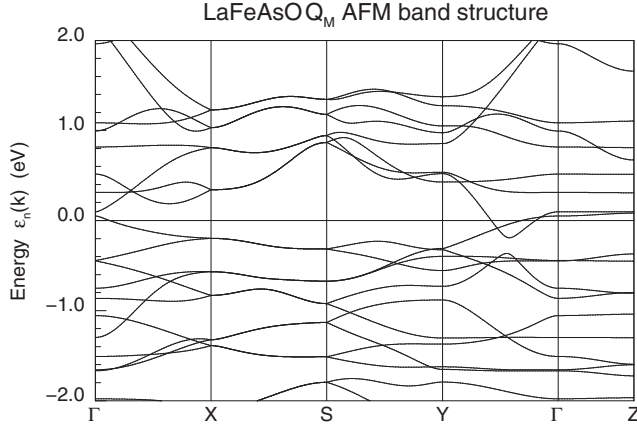


FIG. 3. Band structure of the \bar{Q}_M AFM phase along high symmetry directions. Note that two dispersive bands and one narrow band cross E_F along Γ -Y, while only the one flatter band crosses E_F (very near $k = 0$) along Γ -X.

rotated by 45° from that usually used for the primitive cell; see Fig. 1.)

A striking feature, crucial for accounting for observations, is that the DOS is (roughly) particle-hole symmetric, as is the observed superconducting behavior. All bands near E_F are essentially 2D, resulting in only slightly smeared 2D-like DOS discontinuities at the band edges with structure elsewhere due to band crossings and non-parabolic regions of the bands. The DOS has roughly a constant value of 0.25 states/(eV Fe spin) within 0.15–0.2 eV of E_F , with much flatter bands beyond. The hole and electron effective in-plane masses, obtained from $N(E) = m^*/(\pi\hbar^2)$ for each pocket, are $m_h^* = 0.33$, $m_e^* = 0.25$. A related band structure occurs in electron-doped HfNiCl [38], but there superconductivity appears before the heavy bands are occupied.

While linear electron-phonon coupling in the nonmagnetic phase has been calculated to be weak [39,40], we find that strong *magneto* phonon coupling arises in this system (Fig. 5): the Fe moment changes at a rate of $6.8 \mu_B/\text{\AA}$ as the Fe-As distance is varied (by changing the As layer height). This unusually large sensitivity of the moment to the local structure sets the LaFeAsO system apart from other magnetic superconductors. Figure 5 also reveals another important aspect: LDA and GGA are almost 0.1 \AA off in predicting the height of the As layer relative to Fe, a discrepancy that is uncomfortable large. Neglecting the Fe magnetism increases the discrepancy.

“Doping” (change of charge in the FeAs layers) is observed to cause the Néel temperature to decrease, and no magnetic order is apparent in superconducting samples. The effect of (rigid band or virtual crystal) doping on the Q_M electronic structure, either by electrons or holes, is to move E_F into a region of heavier carriers, by roughly an order of magnitude. About 0.08 carriers is sufficient to do this, which is just the amount of doping that results in

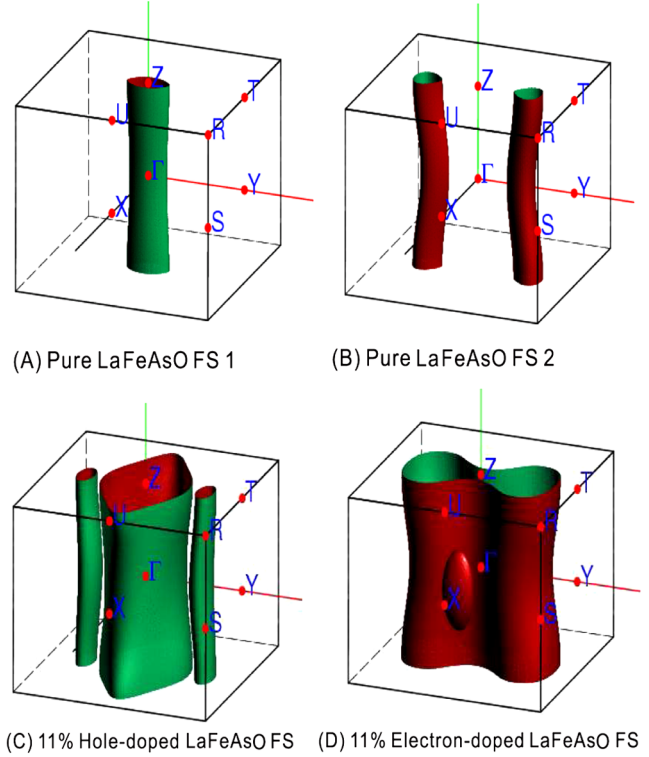


FIG. 4 (color online). Fermi surfaces of LaFeAsO. (a) and (b) the hole cylinders and electron tubes of the stoichiometric Q_M phase. (c) and (d) hole- and electron-doped surfaces.

superconductivity. The evolution of the Fermi surfaces with either sign of doping is pictured in Fig. 4.

The spectrum of magnetic fluctuations is an important property of any AFM phase, and may bear strongly on the emergence of superconductivity. We have calculated from linear response theory the exchange couplings $J_{ij}(q)$ for all pairs $\{i, j\}$ within the unit cell, and by Fourier transform the real space exchange couplings $J_{ij}(R)$, for the transverse spin-wave Hamiltonian [41,42]

$$H = -\sum_{\langle i,j \rangle} J_{ij} \hat{e}_i \cdot \hat{e}_j; \quad J_{ij}(R) = -\frac{d^2 E[\{\theta\}]}{\partial \theta_i(0) \partial \theta_j(R)}, \quad (1)$$

where $\theta_j(R)$ is the angle of the moment (with direction \hat{e}_j) of the j th spin in the unit cell at R . For the Q_M AFM phase and experimental structural parameters, the 1st and 2nd neighbor couplings are (distinguishing coupling for near-neighbor pairs parallel to the spin chains J_1^\parallel and perpendicular to the spin chains J_1^\perp)

$$J_1^\perp = -550 \text{ K}; \quad J_1^\parallel = +80 \text{ K}; \quad J_2^\perp = -260 \text{ K}. \quad (2)$$

For comparison, the nearest neighbor coupling [41,42] in elemental FM Fe is $J_1 \approx 1850 \text{ K}$, i.e., 3–4 times as strong. The signs are all supportive of the actual ordering, there is no frustration. The factor of 7 difference between the two

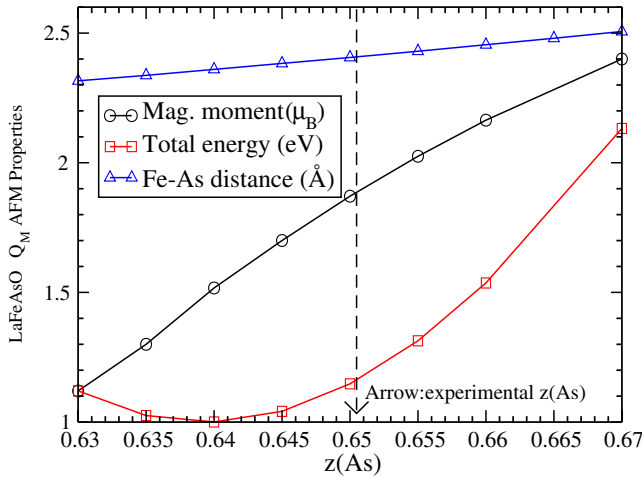


FIG. 5 (color online). The magnitude of the Fe magnetic moment, the change in energy, and the Fe-As distance, as the As height z_{As} is varied.

1st neighbor couplings reflects the strong asymmetry between the x and y directions in the Q_M phase, which is also clear from the bands. The sensitivity to the Fe-As distance is strong: for $z(\text{As}) = 0.635$, where the moment is decreased by 40% (Fig. 5), the couplings change by roughly a factor of 2: $J_1^\perp = -200$ K, $J_1^\parallel = +130$ K, $J_2^\perp = -140$ K. The interlayer exchange constants will be much smaller and, although important for the (three dimensional) ordering, that coupling should leave the spin-wave spectrum nearly two-dimensional.

We emphasize that these exchange couplings apply only to small relative rotations of the moments (spin waves). They cannot be compared to those presented by Yildirim [31] for constrained Fe moments with arbitrary orientations. The $Q = 0$ phase couplings are different from those for the Q_M phase; furthermore, when FM alignment is enforced the magnetism disappears entirely. The magnetic coupling is alignment-dependent, largely itinerant, and as mentioned above, it is sensitive to the Fe-As distance.

The electronic and magnetic structure, and the strength of magnetic coupling, in the reference state of the new iron arsenide superconductors has been presented here, and the origin of the electron-hole symmetry of superconductivity has been clarified. The dependence of the Fe moment on the environment, and an unusually strong magnetophonon coupling, raises the possibility that magnetic fluctuations are involved in pairing, but that it is longitudinal fluctuations that are important here.

W. E. P. thanks Y. Tokura, P. B. Allen, J. W. Lynn, I. I. Mazin, and M. D. Johannes for discussions on this system. We acknowledge support from NSF Grants DMR-0608283 and DMR-0606498 (S. Y. S.) and from NSF Grant DMR-0421810 (W. E. P.). We also acknowledge collaborative work supported by DOE SciDAC Grants DE-FC02-

06ER25793 and DE-FC02-06ER25794. S. L. acknowledges financial support from ANR PNANO Grant ANR-06-NANO-053-02 and ANR Grant ANR-BLAN07-1-186138.

- [1] J. G. Bednorz and K. A. Müller, *Z. Phys. B* **64**, 189 (1986).
- [2] M. J. Geselbracht *et al.*, *Nature (London)* **345**, 324 (1990).
- [3] Y. Maeno *et al.*, *Nature (London)* **372**, 532 (1994).
- [4] K. Takada *et al.*, *Nature (London)* **422**, 53 (2003).
- [5] E. Morosan *et al.*, *Nature Phys.* **2**, 544 (2006).
- [6] S. Yamanaka *et al.*, *Nature (London)* **392**, 580 (1998).
- [7] J. Nagamatsu *et al.*, *Nature (London)* **410**, 63 (2001).
- [8] J. Chaloupka and G. Khaliullin, *Phys. Rev. Lett.* **100**, 016404 (2008).
- [9] Y. Kamihara *et al.*, *J. Am. Chem. Soc.* **130**, 3296 (2008).
- [10] H.-H. Wen *et al.*, *Europhys. Lett.* **82**, 17 009 (2008).
- [11] Z.-A. Ren *et al.*, arXiv:0803.4283.
- [12] Z.-A. Ren *et al.*, *Europhys. Lett.* **82**, 57 002 (2008).
- [13] X. H. Chen *et al.*, arXiv:0803.3603.
- [14] Z.-A. Ren *et al.*, *Europhys. Lett.* **83**, 17 002 (2008).
- [15] P. Cheng *et al.*, *Sci. in China G* **51**, 719 (2008); arXiv:0804.0835.
- [16] A. S. Sefat *et al.*, *Phys. Rev. B* **77**, 174503 (2008).
- [17] G. F. Chen *et al.*, *Phys. Rev. Lett.* **100**, 247002 (2008).
- [18] T. Watanabe *et al.*, *Inorg. Chem.* **46**, 7719 (2007).
- [19] S. Lebègue, *Phys. Rev. B* **75**, 035110 (2007).
- [20] D. J. Singh and M.-H. Du, *Phys. Rev. Lett.* **100**, 237003 (2008).
- [21] H.-J. Zhang *et al.*, arXiv:0803.4487v2.
- [22] I. I. Mazin *et al.*, arXiv:0803.2740v3 [*Phys. Rev. Lett.* (to be published)].
- [23] Q. Han *et al.*, *Europhys. Lett.* **82**, 37 007 (2008).
- [24] X. Dai *et al.*, arXiv:0803.3982v2 [*Phys. Rev. Lett.* (to be published)].
- [25] K. Kuroki *et al.*, arXiv:0803.3325.
- [26] C. Cao *et al.*, *Phys. Rev. B* **77**, 220506(R) (2008).
- [27] F. Ma and Z.-Y. Lu, arXiv:0803.3286 [*Phys. Rev. Lett.* (to be published)].
- [28] T. Li, arXiv:0804.0536.
- [29] Y. Tsujimoto *et al.*, *Nature (London)* **450**, 1062 (2007).
- [30] J. Dong *et al.*, *Europhys. Lett.* **83**, 27 006 (2008).
- [31] T. Yildirim, arXiv:0804.2252.
- [32] C. de la Cruz *et al.*, *Nature (London)* **453**, 899 (2008).
- [33] T. Nomura *et al.*, arXiv:0804.3569.
- [34] P. Blaha *et al.*, *WIEN2K* (Techn. Univ. Wien, Vienna, Austria, 2001).
- [35] K. Koepnik and H. Eschrig, *Phys. Rev. B* **59**, 1743 (1999).
- [36] K. Koepnik *et al.*, *Phys. Rev. B* **55**, 5717 (1997).
- [37] J. P. Perdew and Y. Wang, *Phys. Rev. B* **45**, 13 244 (1992).
- [38] R. Weht *et al.*, *Europhys. Lett.* **48**, 320 (1999).
- [39] L. Boeri *et al.*, *Phys. Rev. Lett.* **101**, 026403 (2008).
- [40] H. Eschrig, arXiv:0804.0186.
- [41] A. I. Liechtenstein *et al.*, *J. Magn. Magn. Mater.* **67**, 65 (1987).
- [42] X. Wan *et al.*, *Phys. Rev. Lett.* **97**, 266403 (2006).